Surface Scanning Analysis with the Laser Antenna Surface Scanning Instrument

Max Mayang Mason, University of Maryland Baltimore County

Advisor: Dr. Pedro Salas, Green Bank Observatory

Summer 2020

Abstract

The surface of the Green Bank Telescope (GBT) is subject to deformations due to heating, wear and tear, and other external factors. These physical deformations do not harm the telescope, and they can be accounted for by using the actuators that are built in between the panels of the dish. However, efficient observations require the shape of the dish to remain as close to a paraboloid. In order to improve the efficiency of the observations, the surface of the telescope is scanned using the laser antenna surface scanning instrument (LASSI). Many small holes exist in between panels, which makes it difficult to accurately measure the deformations. In order to make accurate measurements of these deformations, a mask is applied to any small holes or unwanted artifacts. Once these holes and/or artifacts are masked, the deformations of the primary reflector may be measured with a higher accuracy. In order to determine how to best implement the mask, the author investigated how masking before smoothing affects the measurement of deformations with respect to masking only after smoothing. This was executed by taking residuals between the active surface of the dish and surface scans of the dish, before and after the additional mask was applied. These residuals were compared with different methods of statistical analysis. The residual analysis showed that more masking showed no improvement to the data. This suggests that, given the current data processing, masking is not the limiting factor setting the accuracy of the measured deformations.

1. Background

1.1 Deformations of the Dish

The surface of the Green Bank Telescope (GBT) is made up of 2,004 aluminum panels manufactured to a surface accuracy of better than 50 microns root mean square[1]. Actuators, or small motors used for positional correction, are built into the panels in order to compensate for unintended position changes. Figure 1.1 is an image of the GBT which shows the different panels on its surface.

The surface of the GBT, being a 2.34 acre metal structure in the middle of a field, is subject to physical deformation due to heating, wear and tear, gravity and other external factors. Currently, gravitational deformations of the GBT are well understood and are corrected automatically by the telescope's control system. This makes heating and wind the main contributors to the deformations that need to be measured during an observation. The actuators allow these deformations to be corrected for.

In between the panels of the GBT, there exist small gaps or holes. While examining the effect of deformations on the GBT, these small holes begin to interfere with the analysis, as the large amount of holes in the surface make it difficult to measure the actual deformations in the dish.

1.2 LASSI

Currently, the Green Bank Telescope uses out-of-focus holography to correct for thermal deformations on the surface of the telescope. This method requires frequent recalibration in order to properly make observations at 3mm, which takes approximately 15 minutes to perform and therefore limits when these kinds of observations can be made. By exploring the possibility of using a Terrestrial Laser Scanner, deformations may be able to be measured in near-real time and then corrected using the active surface. The Laser Antenna Surface Scanning Instrument (LASSI) is able to produce a hundred million angle and range measurements of the surface every few minutes.

1.3 Efficiency

Radio telescopes like the GBT are designed with a parabolic shape because all points which lie on the parabola are equidistant from a single focus point. This parabolic shape is what allows for radio observations to be made; as described in figure 1.2, light will enter the dish at all points, the light is then reflected by its surface, or the primary reflector, and captured by a receiver placed at the focal point of the paraboloid allowing all of the light to be captured at a single position at a shared time. However, due to light's behavior as a wave it has a specific phase. If the light is captured at the focus at different phases, the different rays of light will interfere with each other. If there are deviations from the expected parabolic shape in the surface of the dish, the light will asynchronously return to the focus and the efficiency of observations will diminish.

1.4 Zernike Polynomials

While analyzing the results of the surface scans, the metric used to measure the deviations of the dish from the active surface are Zernike polynomials. Zernike polynomials are a sequence of polynomials, where each variable in the series is describing a different kind of deformation. They are useful for describing optical deformations because they are orthogonal over the unit circle and their linear combination is able to reproduce most deformations observed in optical systems. For instance in the LASSI analysis vertical astigmatism may be identified as polynomial Z4. An example of a way Zernike polynomials are defined may be described by figure 1.3. The GBT does not use this model exactly, as the polynomials are in a different order, but it is very similar.

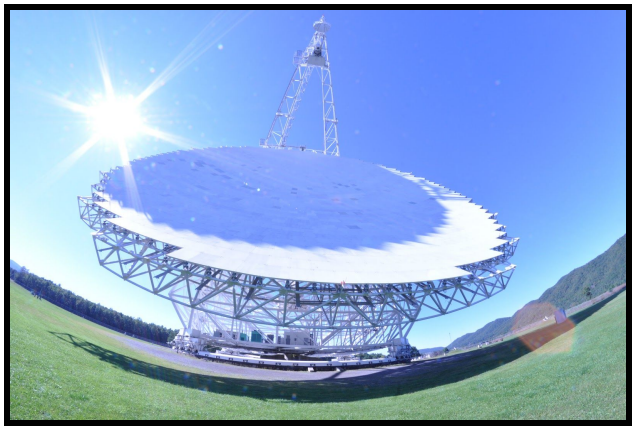

Figure 1.1: A photo of the GBT which shows the different surface panels.

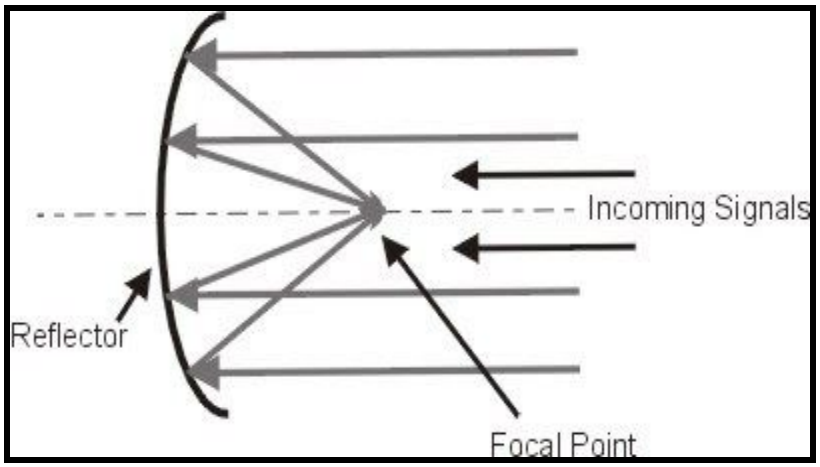

Figure 1.2[2]: An illustration which describes the basic functionality of the components of a radio telescope. Signals enter in the form of light and are reflected by the parabolic surface (primary reflector). The reflected signal is then captured at a receiver placed at the focal point of the parabola.

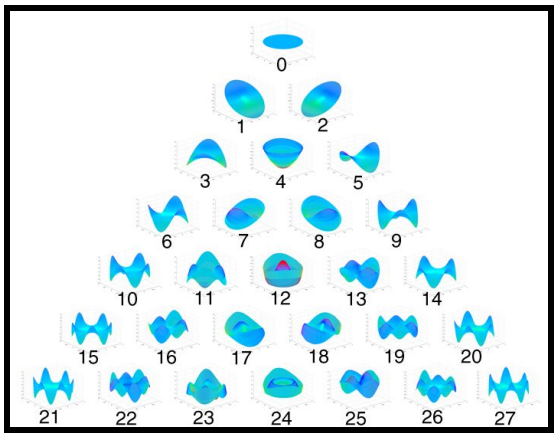

Figure 1.3[3]: An image illustrating how Zernike polynomials may be sequenced to describe physical deformations. Note: this is just an example of concept and the GBT uses a different sequence to describe deformations.

2. Methods

2.1 Smoothing

It is ideal to have a system that measures deformations in near real-time so that they may be corrected with the active surface as quickly and efficiently as possible. There are 10 million position points on the dish of the GBT, a data volume this large takes time to process. In order to make the data set more manageable, it is *smoothed*. The range measurements are averaged using a Gaussian kernel. During the smoothing the coordinates are processed in spherical coordinates so that every smoothed point samples an equal solid angle. The raw data of the surface is taken in in the form of a point cloud, then segmented into a defined object that is the dish. Once when the data is segmented into this object, the gaussian average may be completed and the scan of the dish is smoothed. Figure 2.1 visually describes the process of smoothing.

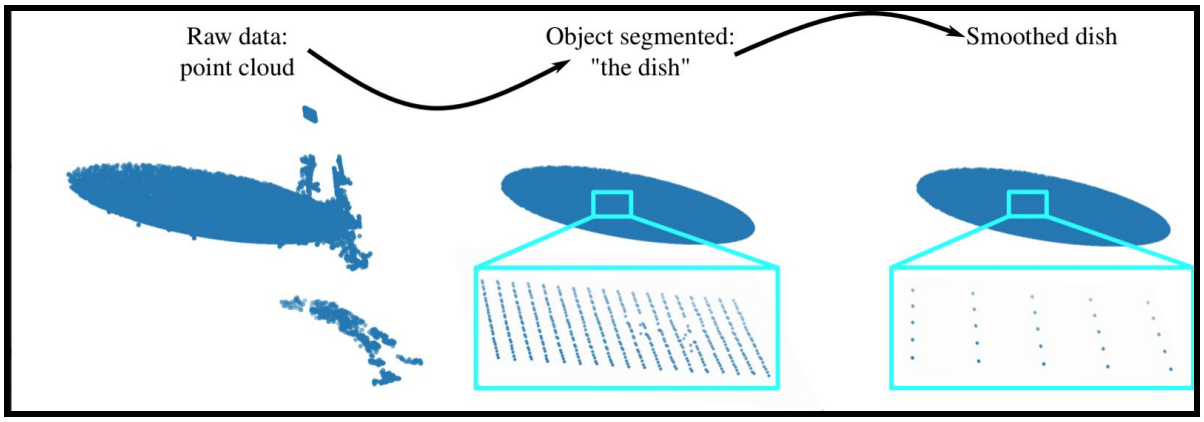

Figure 2.1: A visual description of the process of smoothing. The data is captured in the form of a point cloud. The data is processed into spherical coordinates and segmented into an object defined as the dish. This segmented data is then averaged using a Gaussian kernel. What is left is a smoothed dataset that is more manageable to process.

2.2 Masking

Masking is the process of removing unwanted pieces from a dataset. In order to mask the GBT's surface data, the 3 dimensional position of the telescope is scanned and recorded in the form of 3 arrays: one for the x coordinates, y coordinates and z coordinates of the telescope dish. The coordinate scan data of the telescope is then interpolated into a new Cartesian lattice, of which the paraboloid shape can be fitted to a point cloud. The positions of points are compared to the paraboloid of best fit. Given the properties of the GBT, it is expected that thermal deformations will not exceed a certain value (1.5mm), and any points beyond this threshold will be considered deformed. The points that contain small holes or other unwanted artifacts are excluded, or masked. Anything beyond the small holes are at least 5mm behind the dish and can easily be discarded.

During this investigation, the mask is applied to scans after smoothing takes place. Previous to this, masking was only applied after smoothing is completed. The mask that is applied before smoothing is derived from the masks obtained after smoothing and therefore should be the same mask.

2.3 Pathing

The scans that are masked are in terms of pixels. This is not ideal because the holes and malfunctioning panels are fixed to the surface of the telescope, but their locations on the Cartesian lattice change. It would be beneficial to have the scans in a cartesian format so that a mask may be defined to one scan to one scan, then apply that same mask to a different scan without finding discrepancies in the positions of the holes. These large holes are defined as polygons so that it may be determined if an array of coordinates exist inside of these defined polygons.

Figure 2.1 describes the steps used to define the masks in Cartesian coordinates relative to the telescope's dish. First a mask is applied to a scan to remove all small holes and similarly unwanted artifacts. Then in order to find the boundaries of objects within the scan, a Canny Image Filter, an edge detection operator that uses a multi-stage algorithm to detect a wide range of edges in images[4], is applied to the masked scan, as implemented in scikit.image[5]. The standard deviation of this image filter is then increased until only the edges of large holes on the dish remain. A smoothing kernel is used to remove any additional small holes. What remains are the edges of the large holes that are then defined as polygons.

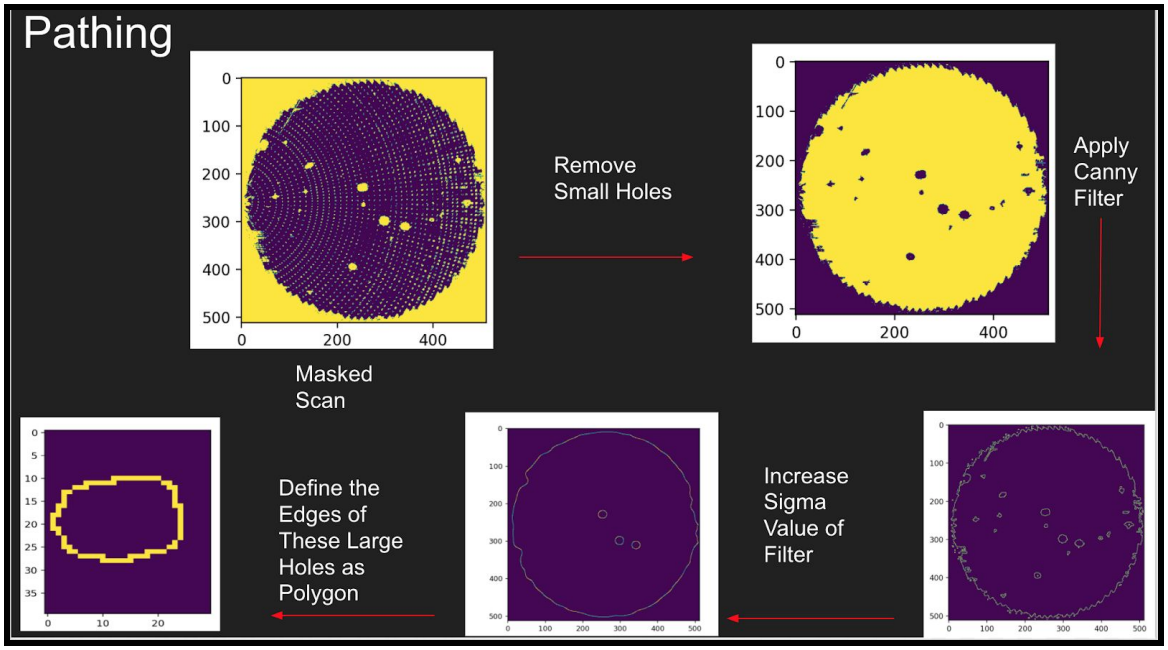

Figure 2.1: An image describing the pathing process to define the masks in Cartesian coordinates relative to the telescope's dish. The steps are as follows: Scan is masked, small holes are removed, Canny Image Filter is applied, standard deviation of filter is increased, edges of large holes are defined as polygons.

3. Results

3.1 Residual Analysis

After smoothing and masking of the surface data, the effects of additional masking before smoothing on measurement of deformations, as opposed to only after, were investigated. It was expected that applying masking before smoothing would improve accuracy. To test the accuracy of LASSI for measuring deformations the active surface is utilized; the active surface is used to deform the surface of the telescope and then the deformations are attempted to be measured using LASSI. This is accomplished by using a pair of scans. The first scan, dubbed a reference scan, is obtained when the active surface is set to reproduce the ideal paraboloid. The second scan, a signal scan, is obtained after the active surface is commanded to deform from the shape of the ideal paraboloid. By taking the difference between these scans LASSI measures deformations of the primary reflector. Since the deformations produced by the active surface are known, they can be compared with the deformations measured by LASSI. In order to test this, the residuals of 16 different unmasked signal scans, each taken at a different time during March 2020, are compared to the reference scan. Those same signal scans were masked and then compared to the reference scan again. What is left are 32 different residual datasets so that 16 different comparisons between unmasked and masked deformations may be performed through different statistical methods. Figure 3.1 shows one of the 16 comparisons of how the deformations are measured in the form of zernike polynomials. The x axis shows the different kinds of deformations that are measured with the scans, while the y axis shows the amplitude of those deformations' occurrence. The pink (input) is what the active surface is showing, while blue (measured) is the scan taken of the telescope's surface. The plot on the left is unmasked while the plot on the right is masked. These plots help show that the unmasked and masked scans yield different amplitudes of deformation compared to the active surface, which shows that masking before smoothing produces different results than masking after smoothing. The results were analyzed by studying the differences between the masked and unmasked scans, which may be seen in Figure 3.2.

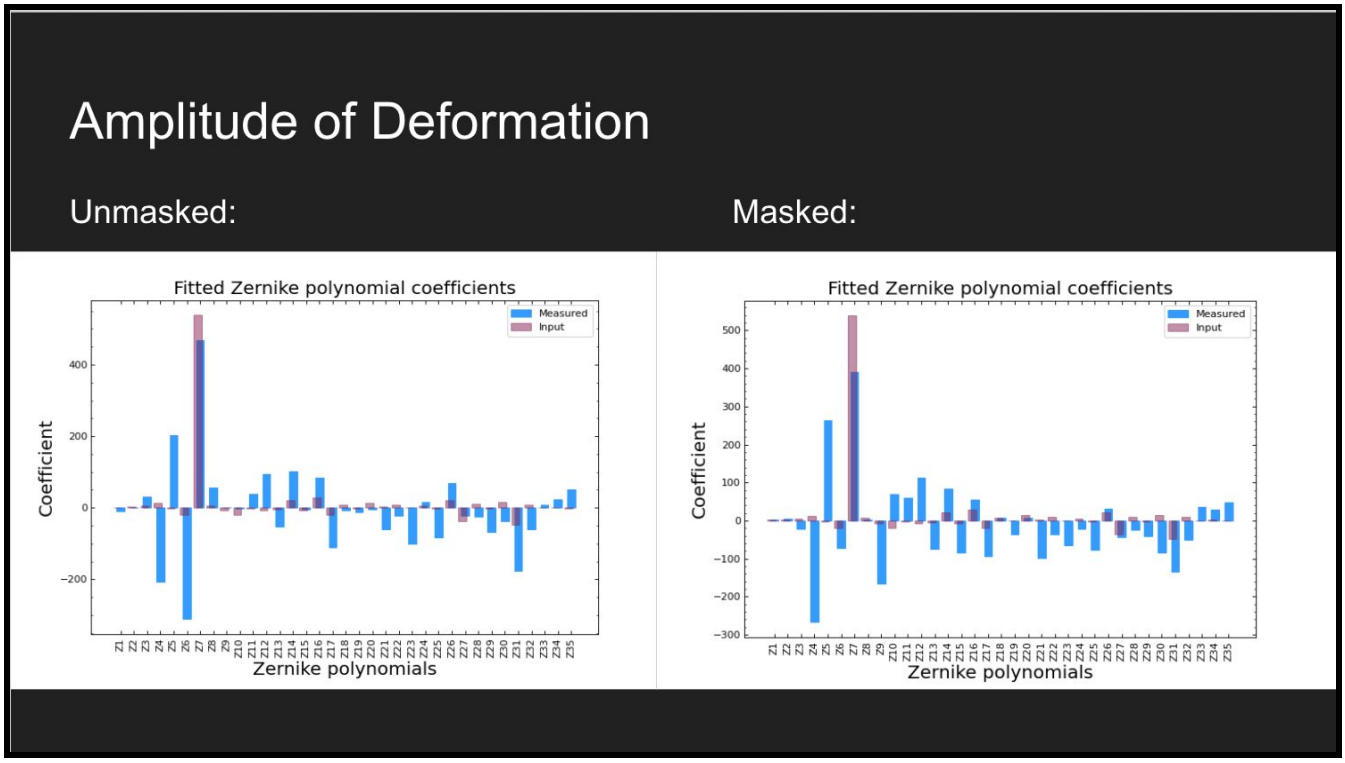

Figure 3.1: Amplitude comparison of Zernike polynomials between an unmasked scan and a masked scan. Pink represents the input of the active surface, while blue represents the measurement of scans taken of the telescope's surface.

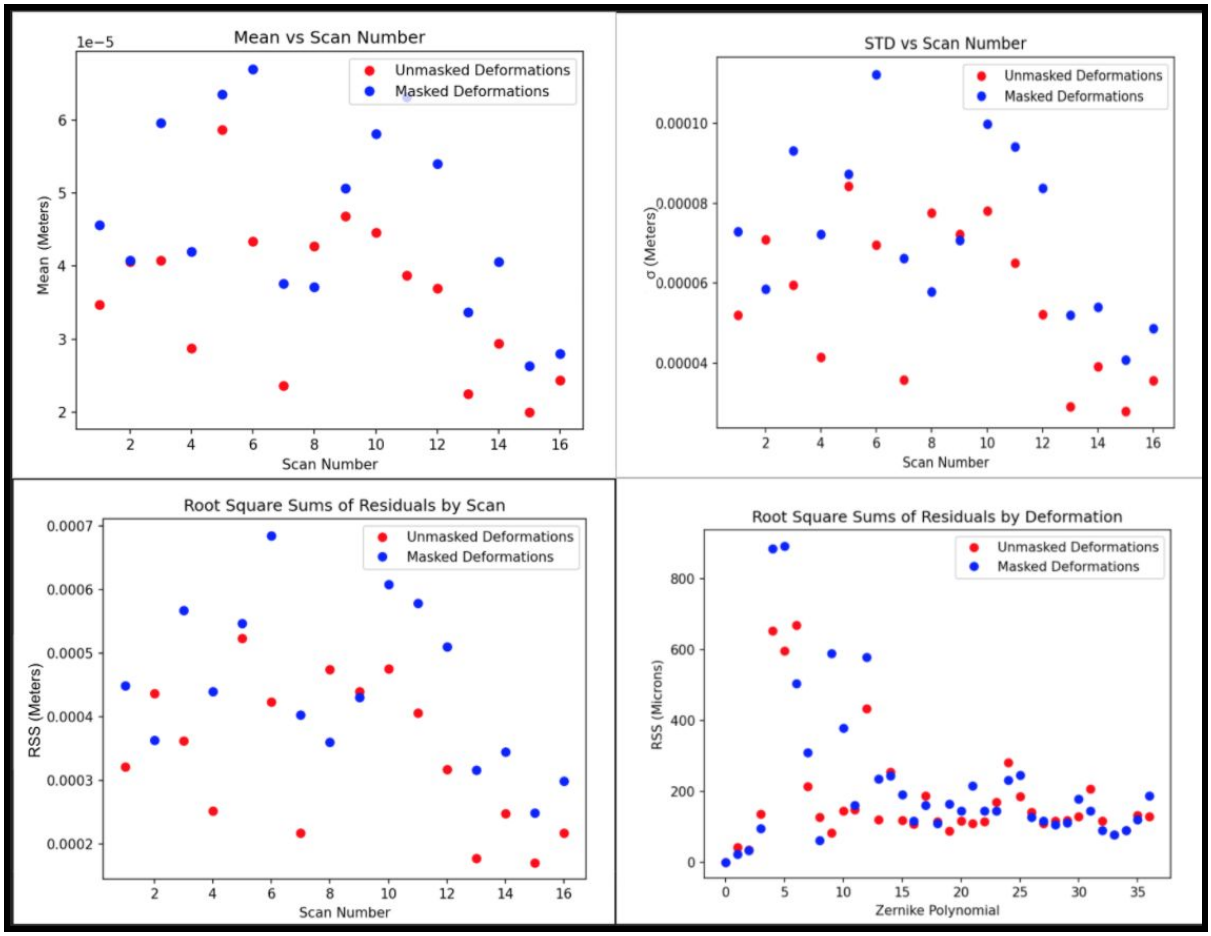

Figure 3.2: Four different plots of residual analysis, comparing the deformation of an unmasked and a masked scan. Red represents the unmasked scan deformations while blue represents masked scan deformations.

The statistical methods used to analyze the residual deformation data of the unmasked and masked signal scans compared to the active surface are mean, standard deviation and root square sum (RSS). RSS is calculated by squaring all of the individual data values in a sample, adding those squared values, and square rooting that sum. RSS measures for the wavefront error, which is directly related to the surface error of the telescope and the aperture efficiency.

In the plot “Mean vs Scan Number” in Figure 3.2, for each scan the amplitude of all 35 Zernike polynomials are averaged together and compared in a scatter plot. The x axis is the number of the scan while the y axis is the mean value of deformation in meters. The most ideal scan would have deformations closest to zero. This plot shows that the amplitude of the mean of the masked deformations tend to be larger than that of the unmasked, however some of the mean values of zernikes are much more similar than others. Such as the masked and unmasked residuals of scan 16 show a difference of less than $0.5e^{-5}$meters, while the values of scan 5 show a difference of almost $2e^{-5}$meters.

In the plot “STD vs Scan Number” in Figure 3.2, for scan, the standard deviation of the amplitude of all 35 Zernike polynomials are compared in a scatter plot. The x axis is the number of the scan while the y axis is the standard deviation of deformation in meters. This plot shows that the general spread of masked deformations are usually greater than the spread of unmasked data for the same kind of deformation. Some of the standard deviations of masked and unmasked deformations are so close they are almost the same in value, such as that of scan 9 or scan 5. The greatest differences in standard deviation are seen scans 5 and 12, almost reaching $2e^{-5}$meter differences.

In the plot “Root Square Sums of Residuals by Scan”, for each scan the RSS of the amplitude of all 35 Zernike polynomials are calculated and compared in a scatter plot. The x axis is the number of the scan while the y axis is the RSS value of deformation in meters. The plot shows that the RSS of masked deformations is usually greater than that of the unmasked data. The amplitude of the difference in RSS between masked and unmasked varies by each kind of deformation. It is notable to see that the RSS of scan 5, the deformation which shows one of the greatest differences in mean and standard deviation value between masked and unmasked has the lowest RSS. This could mean that the reason this deformation yielded such great difference in the previous two plots is due to some sort of error. More research must be done in order to determine why this occurred.

In the plot “Root Square Sum of Residuals by Deformation”, the RSS of alike Zernike values in all scans were taken and compared in a scatter plot. The x axis is the sequence of Zernike polynomials while the y axis is the RSS value of its deformation in microns. This plot shows that more often the RSS of masked deformations are usually greater than that of the unmasked deformations. However, compared to the previous residual analysis, the RSS by kind of deformation the values of masked deformations were less than that of the unmasked deformations much more frequently and the differences between masked and unmasked deformations are much more similar. Between the ranges of Z20 and Z35, the RSS values are almost exactly the same.

4. Residual Analysis Conclusion

Although it was expected that applying masking before smoothing would improve accuracy, the results show masking before smoothing does not seem to provide significant improvement as opposed to after. This could be because masking is not the most important factor in setting the accuracy with which LASSI can measure deformation.

One possible cause of the residual data showing no improvement is perhaps the mask was not defined well enough; too much or too little of the data was excluded.

Another possibility is there exists unexpected problems during the interpolation of the surface data. At some point during processing after smoothing, the spherical surface data is converted to a cartesian due to the weight of a cartesian system being more uniform. This is executed by using a linear interpolation between the spherical and Cartesian systems. Due to the large amount of data being masked and interpolated, improvement to the ability to measure deformations could have been limited.

If there were more time to investigate the problem further, the limiting factor may be determined. The cause behind why additional masking does not provide significant improvement is a subject for future research on the topic.

Acknowledgments

The author would like to thank his research advisor Dr. Pedro Salas for consistent guidance and support for the duration of the project. Dr. Andrew Seymour for assistance in understanding various aspects of the project. Dr. Marty Bloss for introducing the summer opportunity to the author. Dr. Will Armentrout for site overview of the summer programs at the GBT. NRAO, PING, and GBO for offering this amazing opportunity for students interested in radio astronomy.

References

[1] Prestage, R. M.; Constantikes, K. T.; Hunter, T. R.; King, L. J.; Lacasse, R. J.; Lockman, F. J.; Norrod, R. D. *The Green Bank Telescope*. Proceedings of the IEEE. Volume 97, Issue 8, Aug. 2009, p. 1382-1390

[2] ITSO, *Day 1 Session 2.* INTERNATIONAL TELECOMMUNICATIONS SATELLITE ORGANIZATION, n.d.

[3] Twa, Michael & Parthasarathy, Srinivasan & Raasch, Thomas & Bullimore, Mark. (2003). Decision Tree Classification of Spatial Data Patterns From Videokeratography Using Zernike Polynomials. 10.1137/1.9781611972733.1.

[4] Canny, J., A Computational Approach To Edge Detection, IEEE Transactions on Pattern Analysis and Machine Intelligence, 8(6):679–698, 1986.

[5] Stéfan van der Walt, Johannes L. Schönberger, Juan Nunez-Iglesias, François Boulogne, Joshua D. Warner, Neil Yager, Emmanuelle Gouillart, Tony Yu and the scikit-image contributors. scikit-image: Image processing in Python. PeerJ 2:e453 (2014) https://doi.org/10.7717/peerj.453